PHYSICAL REVIEW LETTERS

Nonlinear Terahertz Response of *n*-Type GaAs

P. Gaal,[1] K. Reimann,[1,*] M. Woerner,[1,†] T. Elsaesser,[1] R. Hey,[2] and K. H. Ploog[2]

[1]*Max-Born-Institut für Nichtlineare Optik und Kurzzeitspektroskopie, 12489 Berlin, Germany*
[2]*Paul-Drude-Institut für Festkörperelektronik, 10117 Berlin, Germany*

Excitation of an *n*-type GaAs layer by intense ultrashort terahertz pulses causes coherent emission at 2 THz. Phase-resolved nonlinear propagation experiments show a picosecond decay of the emitted field, despite the ultrafast carrier-carrier scattering at a sample temperature of 300 K. While the linear THz response is in agreement with the Drude response of free electrons, the nonlinear response is dominated by the super-radiant decay of optically inverted impurity transitions. A quantum mechanical discrete state model using the potential of the disordered impurities accounts for all experimental observations.

The interplay of carriers in localized and delocalized states is essential for the optical and transport properties of semiconductors. In *n*-type III-V materials, shallow donor impurities with an electron binding energy E_B of a few meV, e.g., Si, ionize at elevated temperature T, thus providing free electrons in conduction band states. Scattering of free electrons with ionized impurities determines electron mobility to a large extent and is relevant for the far-infrared optical properties. Two regimes of materials response have been identified:

(i) For $kT \gg E_B$ (k is the Boltzmann's constant), the frequency dependent conductivity is well described by the Drude theory [1], which considers a quasifree electron gas with a mean momentum relaxation time τ_{Drude}, resulting in a *homogeneously* broadened Lorentzian absorption band centered at the frequency $\nu = 0$ [2,3].

(ii) At very low doping concentrations ($N \lesssim 10^{14}$ cm^{-3}) and at low temperatures, studies of optical transitions between donor electron states in the THz range [4–6] have revealed nanosecond population lifetimes and picosecond decoherence times of coherent polarizations. Such properties are the basis for far-infrared lasers based on donor transitions in Si [7]. They also make donors candidates for charge qubits in quantum information processing [8–11].

Regime (i) is characterized by completely delocalized wave functions of continuum states, whereas localized wave functions on impurity sites are essential in regime (ii). In the intermediate and high doping range ($N \gtrsim 10^{16}$ cm^{-3}) at room temperature, both localized and delocalized electrons exist, resulting in a complex dynamic behavior that is to a large extent not understood. Linear [12] and nonlinear spectroscopy [13] in the THz frequency range represents a particular powerful tool to explore such phenomena.

In this Letter, we study the nonlinear THz response of *n*-type bulk GaAs at $T = 300$ K and report the first observation of a long-lived coherent THz emission excited by intense ultrashort THz pulses with electric field amplitudes up to 70 kV/cm. The emission is centered at 2 THz and displays a picosecond decoherence time, in sharp contrast to the Drude scattering time $\tau_{\mathrm{Drude}} = 150$ fs derived from the linear THz response of the sample. The emitted THz field is due to phase-coherent stimulated emission from impurities having a populated excited state and an unpopulated ground state (inversion). A quantum mechanical discrete state model describing the disordered impurity potential accounts for such behavior.

The sample investigated consists of a 500 nm thick layer of Si-doped GaAs with a doping concentration of $N_{\mathrm{Si}} = 10^{17}$ cm^{-3}. The layer was grown by molecular beam epitaxy between two 300-nm thick Al$_{0.4}$Ga$_{0.6}$As barriers [14] on a 500 μm thick semi-insulating GaAs substrate. Linear THz experiments were performed with the sample as grown. For nonlinear propagation studies the substrate was removed by wet chemical etching [15]. In the experiments, the sample was excited by few-cycle THz pulses in the 1–5 THz range, using our novel source for high-amplitude THz transients [16]. The transmitted THz field was measured in amplitude and phase by electro-optic sampling [17] in a ZnTe crystal. The setup of the nonlinear propagation experiment is similar to that of [13]. All experiments were performed at room temperature in a dry nitrogen atmosphere.

The linear THz response of the sample was studied in a parallel THz beam of low intensity [cf. inset of Fig. 1(a)]. Figure 1(a) shows the measured transients of the incident $E_{\mathrm{in}}(t)$ (dashed line) and the transmitted THz field $E_{\mathrm{out}}(t)$ (dots) after correcting for the dispersion introduced by the GaAs substrate. The transmitted pulse displays a reduced amplitude due to reflection and a small negative phase shift. The decrease in amplitude is dominated by the reflection losses from the sample surfaces. The solid line in Fig. 1(a) shows the transmitted pulse calculated with the Drude model with a scattering time of $\tau_{\mathrm{Drude}} = 150$ fs, in excellent agreement with the experimental curve. Previous experiments in the linear regime have demonstrated a similar behavior of *n*-type GaAs at somewhat lower dop-
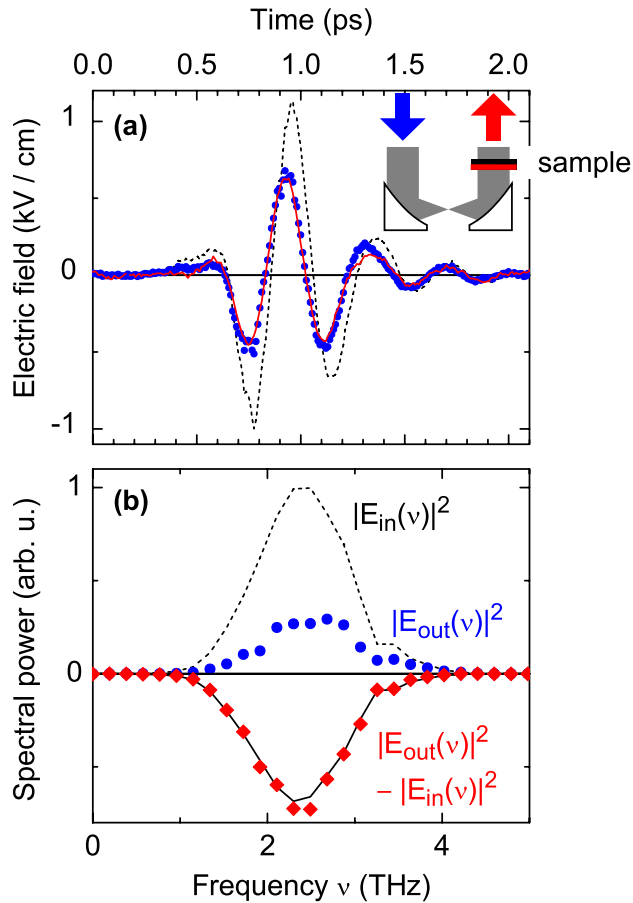
FIG. 1 (color online). (a) Linear propagation of THz pulses through an *n*-type GaAs layer. The electric field is plotted as a function of time for the incident pulse $E_{in}(t)$ (dashed line) and for the transmitted pulse $E_{out}(t)$ (dots). The expected $E_{out}(t)$ according to the Drude model including reflection losses at the surfaces is shown for comparison (solid line). Inset: Experimental setup for the linear regime. (b) Corresponding power spectra. Diamonds, measured difference $|E_{out}(\nu)|^2 - |E_{in}(\nu)|^2$. Solid line, the expected Drude result.

FIG. 2 (color online). Nonlinear propagation of THz pulses through the *n*-type GaAs layer without the substrate. (a) Dashed line, incident pulse $E_{in}(t)$; solid line, transmitted pulse $E_{out}(t)$. (b) Corresponding power spectra. Inset: experimental setup. (c) The difference signal $E_{out}(t) - E_{in}(t)$ shows weakly damped oscillations at a frequency of $\nu = 2$ THz. (d) The difference of the power spectra (diamonds) exhibits a pronounced, *positive* peak at 2 THz—in distinct contrast to the expected result from Drude theory (solid line).

ing concentrations [2]. The Fourier transforms of the transients are shown in Fig. 1(b). The difference spectrum $|E_{out}(\nu)|^2 - |E_{in}(\nu)|^2$ (diamonds) is slightly redshifted relative to that of the driving pulse (dashed line) without any spectrally narrow features.

Data recorded in the nonlinear regime of THz response are summarized in Figs. 2 and 3. In such measurements, the sample without the substrate was placed in the focus of two parabolic mirrors [inset of Fig. 2(b)]. Since the thickness of the layer is much smaller than the wavelength of the THz pulse, the waves reflected at the front and rear surfaces of the sample interfere destructively, leading to very low reflection. Figure 2(a) shows the sample response for a driving field amplitude of $E_{max} = 45$ kV/cm. At late times, the transmitted field [solid line in Fig. 2] exhibits a weakly damped component oscillating with a frequency $\nu = 2$ THz, which is the prominent feature in the difference signal $E_{out}(t) - E_{in}(t)$ [Fig. 2(c)]. The cor-
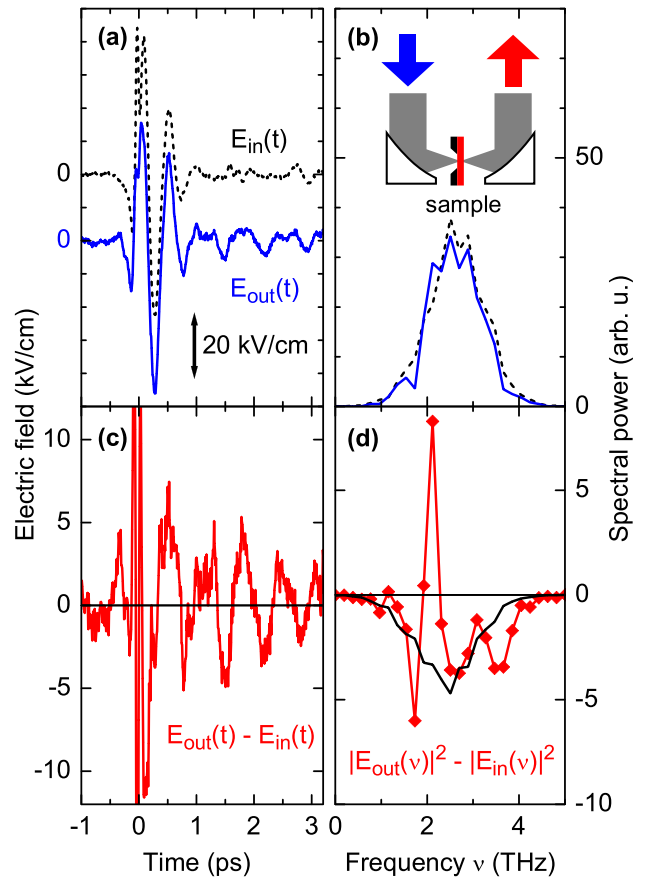
responding power spectra are shown in Figs. 2(b) and 2(d). $|E_{out}(\nu)|^2$ and $|E_{in}(\nu)|^2$ are of similar amplitude, their difference (diamonds) exhibits a pronounced positive peak at 2 THz due to the coherent emission, and negative components due to THz absorption. This behavior is in striking contrast to the Drude response of free electrons (solid line).

In Fig. 3(a), the difference signal $E_{out}(t) - E_{in}(t)$ is plotted for various amplitudes E_{max} of the incident THz pulse. We concentrate on the oscillatory signal after the exciting pulse (the parts of the transients shown as solid lines), the Fourier transforms of which are shown in Fig. 3(b). Oscillations are absent for $E_{max} = 32$ kV/cm (the weak structure around 2.8 ps is an unintentional pulse replica). For $E_{max} \geq 51$ kV/cm, clear oscillations are found, which give rise to the 2 THz peak in the spectrum. In Fig. 3(c), the spectral power of the oscillation around 2 THz (dots) is plotted as a function of E_{max}^2 (dashed line: linear dependence). The nonlinear response increases
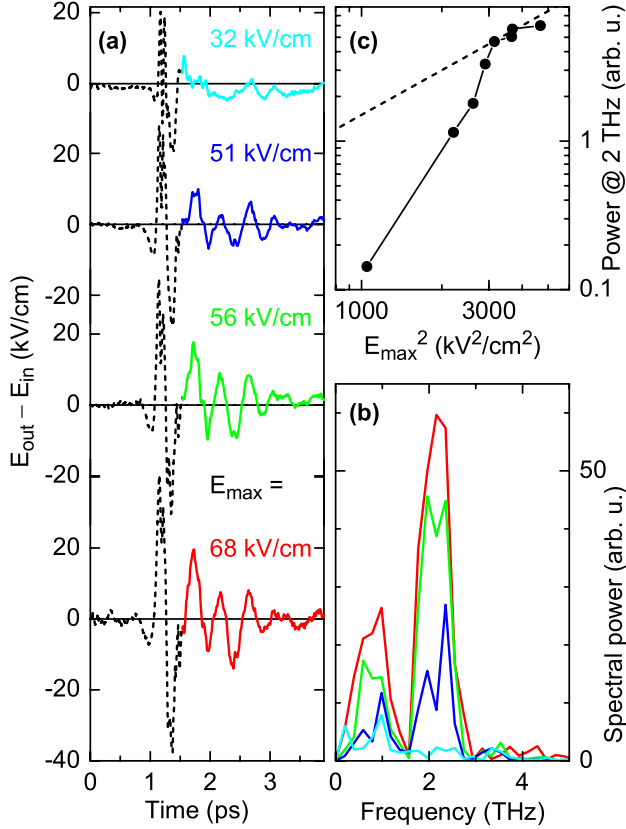
FIG. 3 (color online). (a) Difference signals $E_{out}(t) - E_{in}(t)$ for several amplitudes E_{max} of the incident THz pulse. The coherent oscillations after the main pulse (solid lines) occur above a threshold of $E_{max} \approx 40$ kV/cm. (b) Fourier transforms of $E_{out}(t) - E_{in}(t)$ after the main pulse. (c) Dots: Spectral power at 2 THz as a function of E_{max}^2. For comparison, the dashed line shows a linear dependence.

superlinearly with the field amplitude and saturates at very high driving fields.

The coherent THz emission is absent when the sample is excited with THz pulses not containing frequency components above 1.5 THz. Furthermore, a geometrically identical sample with a lower doping concentration of $N_{Si} = 2 \times 10^{16}$ cm^{-3} does not show any coherent emission when studied under identical excitation conditions.

Now, we discuss the physical mechanisms underlying the long-lived coherent emission—an observation in distinct contrast to the Drude theory of intraband electron response. The transverse THz driving field leads to an in-plane excitation of electrons in the GaAs layer [18]. The THz spectra in the nonlinear regime [diamonds in Fig. 2(d)] demonstrate a nonresonant absorption of the incident THz pulse and a phase-coherent THz emission with a predominant spectral component at 2 THz. The long coherence time of the emission suggest that electronic resonances related to the impurities play an important role for this behavior.

At the doping concentration $N_{Si} = 10^{17}$ cm^{-3} of our sample, the equilibrium electron distribution follows a

Boltzmann statistics with a significant ($\approx 30\%$) fraction of donors neutral at room temperature. Thus, photoinduced ionization and subsequent recombination of impurities contribute to the THz response of the sample. The driving pulse has sufficient field strength to ionize neutral donors by transferring initially bound electrons from the S-like ground state to continuum states, in this way generating additional impurities with an unpopulated ground state. Under such nonequilibrium conditions, the electron gas thermalizes by carrier-carrier scattering on a subpicosecond time scale and populates both high-lying impurity states and the continuum, i.e., conduction band states. In impurities with a populated P-like excited state and an unpopulated ground state, stimulated THz emission can occur on the corresponding dipole-allowed optical transition, which overlaps with the spectrum of the THz driving pulse. As a result, the THz pulse saturates the optical gain within a few picoseconds, leading to the emission of a super-radiant phase-coherent electromagnetic wave. This model also explains the observed dependence on E_{max}. For low E_{max}, the field amplitude is too low for efficient ionization. For high E_{max}, the coherent emission saturates, since at most all electrons can emit coherently.

To support this explanation, we performed model calculations of electronic states in a disordered impurity potential. The single particle Schrödinger equation was numerically solved with the Coulomb potentials of 30 randomly distributed positively charged donors in a $67 \times 67 \times 67$ nm^3 box with periodic boundary conditions. The static dielectric constant $\epsilon_s = 12.4$ and effective electron mass $m_{eff} = 0.067 m_0$ of GaAs correspond to an effective Bohr radius of $a_B = 10$ nm and to an effective Rydberg energy of $E_{Ry} = 6$ meV.

For such parameters, an isolated hydrogenlike impurity displays an $1S \leftrightarrow 2P$ transition frequency of ≈ 1 THz (4 meV), as experimentally observed in far-infrared luminescence experiments [4]. For the doping density in our sample, the average distance between donors is around 20 nm, i.e., of the same order of magnitude as the Bohr radius. Thus, wave functions of neighboring impurities partially overlap, resulting in a delocalization of electron states [19]. This tendency towards delocalization is partially compensated for by the Anderson localization [20] caused by the random distribution of impurities. The effect of these two opposing tendencies is that more than 80% of the donors have a $1S$ ground state wave function strongly localized on the impurity site. The first excited states are much less localized. All other states of the disordered impurity potential are delocalized among all impurities and form a continuum [Fig. 4(c)].

Since the energy levels depend on the number and distance of neighboring impurities, one gets a broad distribution of $1S \leftrightarrow nP$ transition frequencies [Fig. 4(a)]. While this distribution starts at 0.5 THz, below the $1S \leftrightarrow 2P$ transition frequency of isolated impurities (1 THz), the high doping density shifts the center of gravity of the distribution to higher frequencies.
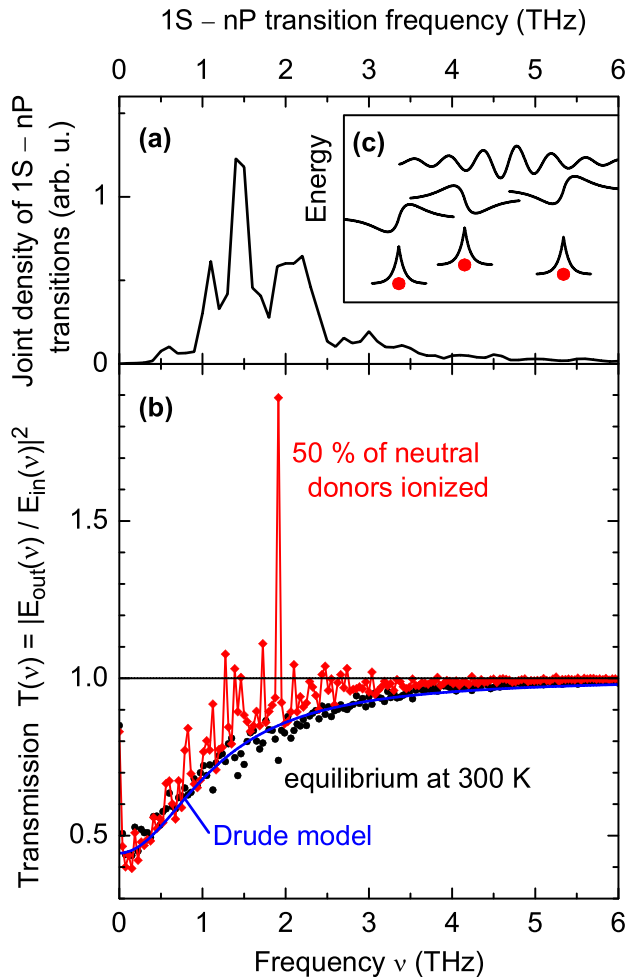
FIG. 4 (color online). Results of solving the single particle Schrödinger equation with the Coulomb potentials of randomly distributed impurities. (a) The solid line shows the joint density of states as a function of the energy difference between the ground state and excited states. (b) Dots, calculated transmission spectrum of the *n*-type GaAs layer at room temperature from our quantum mechanical model, which reproduces very well the result from the Drude model (solid line). Diamonds, ionization of half the neutral donors results in a pronounced gain around 2 THz. (c) Sketch of typical wave functions in the potential of disordered impurities.

This model gives the THz transmission spectra $T(\nu)$ of a 500 nm thick *n*-type GaAs layer shown in Fig. 4(b). The dots were calculated for an equilibrium electron population at room temperature. In equilibrium, 30% of the electrons are in donor ground states. The numerical result fits almost perfectly the analytical result of the Drude model (solid line) and the measured linear optical response of the system (cf. Fig. 1).

The diamonds in Fig. 4(b) show the numerical result of the discrete state model for a nonequilibrium situation, in which half of the initially neutral donors have been ionized by transferring electrons to continuum states. Now, the transmission spectrum $T(\nu)$ exhibits a series of transition lines. The most prominent feature is the optical gain around 2 THz, which is due to the population inversion on donors with one electron in a *P*-like excited state.

In conclusion, we have demonstrated the nonlinear optical response of *n*-type bulk GaAs in the THz range, which is distinctly different from the linear Drude-like behavior. Excitation with strong THz pulses results in coherent emission on impurity transitions with surprisingly long decoherence times. Ultrafast electron redistribution in higher lying impurity states and the conduction band continuum is essential for establishing a population inversion in impurity atoms with an unpopulated ground state. The nonlinear phenomena demonstrated here may lead to novel THz emitters and optical switches.

*Electronic address: reimann@mbi-berlin.de
†Electronic address: woerner@mbi-berlin.de

[1] P. Drude, Ann. Phys. (Berlin) **1**, 566 (1900); **3**, 369 (1900); **7**, 687 (1902); **14**, 667 (1904); **14**, 936 (1904).
[2] N. Katzenellenbogen and D. Grischkowsky, Appl. Phys. Lett. **61**, 840 (1992).
[3] C. Sirtori *et al.*, Appl. Phys. Lett. **75**, 3911 (1999).
[4] I. Melngailis *et al.*, Phys. Rev. Lett. **23**, 1111 (1969).
[5] K.-M. C. Fu *et al.*, Phys. Rev. Lett. **95**, 187405 (2005).
[6] M. F. Doty *et al.*, Phys. Rev. B **71**, 201201(R) (2005).
[7] S. G. Pavlov *et al.*, Phys. Rev. Lett. **84**, 5220 (2000).
[8] B. E. Cole *et al.*, Nature (London) **410**, 60 (2001).
[9] D. G. Allen, M. S. Sherwin, and C. R. Stanley, Phys. Rev. B **72**, 035302 (2005).
[10] X. Hu, B. Koiller, and S. Das Sarma, Phys. Rev. B **71**, 235332 (2005).
[11] B. Koiller, X. Hu, and S. Das Sarma, Phys. Rev. B **73**, 045319 (2006).
[12] R. Huber *et al.*, Phys. Rev. Lett. **96**, 017402 (2006).
[13] C. W. Luo *et al.*, Phys. Rev. Lett. **92**, 047402 (2004).
[14] The AlGaAs layers serve only as etch stops for the etching of the substrate; confinement effects on the GaAs layer are unimportant.
[15] J. J. LePore, J. Appl. Phys. **51**, 6441 (1980).
[16] T. Bartel *et al.*, Opt. Lett. **30**, 2805 (2005).
[17] Q. Wu and X.-C. Zhang, Appl. Phys. Lett. **71**, 1285 (1997).
[18] Under such conditions, the in-plane wave vector is very small and the two-dimensional plasma frequency of the electron gas approaches zero.
[19] F. Stern and R. M. Talley, Phys. Rev. **100**, 1638 (1955).
[20] P. W. Anderson, Phys. Rev. **109**, 1492 (1958).